Low fouling conditions in dead-end filtration: Evidence for a critical filtered volume and interpretation using critical osmotic pressure

Y. Bessiere [a,1], N. Abidine [b], P. Bacchin [a,*]

[a] *Laboratoire de Génie Chimique, Université Paul Sabatier, 118 route de Narbonne, 31062 Toulouse Cedex, France*
[b] *Aquasource, 20 Avenue Didier Daurat, BP 4050, Toulouse Cedex 4, France*

Abstract

This paper presents experiments showing the existence of a critical filtered volume (CFV) when operating colloid dead-end filtration. The CFV is here defined as the filtered volume below which there is no irreversible (with respect to a break in the filtration) fouling on the membrane surface: it has thus the same meaning as cross-flow critical flux but applied to a dead-end process. The existence of the CFV is demonstrated when filtering stable latex or clay suspensions in constant-flux filtration experiments with alternating rinses: in contradiction to the current view, an irreversible deposit is not formed as soon as dead-end filtration begins. This critical filtered volume is shown to be dependent on the suspension stability and to be fully linked to the permeate flux: for permeate fluxes of 80 and $110 \, l \, h^{-1} \, m^{-2}$ the CFV is, respectively, 82 and $651 \, m^{-2}$ for latex particles. Analyses of results are made by depicting the transition between concentration polarisation and deposit formation considering a critical osmotic pressure, which appears to be a characteristic of the fouling potential of a suspension. The results are discussed in the light of how this concept could lead to an interesting way to control and develop a strategy to operate filtration in dead-end mode.
© 2005 Elsevier B.V. All rights reserved.

Keywords: Critical conditions; Osmotic pressure; Fouling test; Deposit formation; Dead-end filtration

1. Introduction

The rapid development of separation systems using membranes made it possible to use pressure-driven processes in a large range of industrial applications. Thus, ultrafiltration is now the principal step in potable water production. For such a low added-value product, costs have to be minimized. Therefore, membrane manufacturers started to develop dead-end units, which proved to lead to energy efficient systems [1].

For both cross-flow and dead-end mode, fouling represents a real limitation. Indeed, this phenomenon, attributed as much to adsorption as to gel formation or particle deposition, leads to an unavoidable rise in production costs by in-

creasing both the energy consumption (to maintain a constant flux) and the cleaning frequencies (backwashes or chemical cleaning). Thus, understanding fouling phenomena and developing ways to anticipate and control them rapidly proved to be essential for the development of water treatment technologies and other applications.

The concept of critical flux has been defined for cross-flow filtration as the flux below, which a decline of permeability with time does not occur [2,3]. The critical flux and its consequences on how filtration should be operated have been experimentally studied for various suspensions [4], membranes [5] and operating conditions [6]. These critical conditions are linked to the idea of sustainable development for a process by defining operating conditions for which fouling is minimised, thus needing little energy to remove it.

Since membrane manufacturers have managed to decrease membrane prices, it became possible to explore low-flux operation with large membrane surfaces leading to the same

* Corresponding author. Tel.: +33 5 61 55 81 63.
E-mail addresses: bessiere@chimie.ups-tlse.fr (Y. Bessiere),
bacchin@chimie.ups-tlse.fr (P. Bacchin).
[1] Tel.: +33 5 61 55 81 63.

or to lower global production costs by saving energy. To optimize operating conditions leading to the best compromise between cost and productivity, research has focused on the development of procedures allowing the determination of running parameters leading to low-fouling operations. In this way, part of the project MemEau coordinated by the Aquasource company (Toulouse, France) focuses on the determination of low fouling conditions in dead-end filtration for water treatment applications.

It is reasonable to assume that an extensive use of membranes under critical conditions (as opposed to intensive use with high pressures or high fluxes associated to heavy fouling) can be an essential key toward sustainable operations.

The focus of the work presented here is to investigate the possibility of avoiding or limiting irreversible fouling in dead-end filtration by using rinses, which do not lead to high-energy losses unlike backwashes. This implies that the limit between the different fouling mechanisms has to be clearly identified.

2. Background

Accumulation of colloidal matter on the membrane surface is inherent to the separation process; it can be limited but never totally avoided. However, accumulation can lead to different fouling mechanisms (pore blocking or blinding, adsorption, cake formation, concentration polarisation [7]) having different consequences on the permeate flux and different degrees of reversibility. Here, we consider the case where fouling is mainly controlled by surface mechanisms and not by internal fouling. Even if surface accumulation has most often been studied as a global cake, some authors [8,9] found that the colloidal deposit can be considered as a combination of a loose reversible layer (concentration polarization) and an irreversible packed structure (gel or deposit layer).

2.1. Concentration polarization

During filtration, particles can remain in a dispersed phase forming a concentrated polarized layer. They provide an additional opposition to transfer via the contribution of the osmotic pressure; when associating this contribution with Darcy's law, the flux (J) can then be described as a function of transmembrane pressure (ΔP), osmotic pressure at the interface between membrane and suspension (Π_m), fluid viscosity (μ) and resistance of the membrane (R_m):

$$J = \frac{\Delta P - \Pi_m}{\mu R_m} \tag{1}$$

Osmotic pressure, which is well known as the limiting phenomenon during reverse osmosis of salt solution, always has a significant effect on colloidal dispersion ultrafiltration [10]: 100 nm particles can exhibit osmotic pressure around 0.2 bars when concentrated as experimentally shown [11]. Authors working on physical aspects of concentrated colloidal dispersions [12] show that a critical osmotic pressure exists, Π_{crit} (for a critical volume fraction) above which there is aggregation between dispersed particles. During separation, the critical osmotic pressure can be reached on the membrane leading to the formation of layers of irreversibly aggregated particles.

2.2. Irreversible fouling layer formation

The formation of colloidal irreversible fouling layers is the consequence of the fact that concentration polarisation reaches its maximum capacity.

At the membrane surface this can mean:

- A critical volume of matter leading to a critical osmotic pressure from a thermodynamic point of view.
- A critical force balance implying that dispersive repulsion forces between solutes or particles are counter-balanced by convective drag forces (summing the drag forces of all the accumulated particles [8]) from a mechanistic point of view.

The idea of a critical concentration is well known since 1968, when it was introduced by Michaels into the gel model [13] and it is often used in developing transient models for molecular filtration [14]; but it is not a concept traditionally used for colloids which are usually considered as particles, to be described by a cake filtration approach implying formation of a deposit as soon as matter accumulates at the surface. However, it is important, at this point, to accept that even with colloid particles there can be a critical concentration as shown by Jönsson and Jönsson in 1996 [12] with a thermodynamic approach and by Petsev et al. in 1993 with a critical force balance [15]; above this critical point, irreversible multilayers of aggregated colloidal particles can then form on the membrane surface, something like a gel or a deposit layer [16]. Such a mechanism then causes additional resistance (R_c) to the filtration which is irreversible. Logically, during its formation there is always a concentrated polarised layer at the surface at its maximum concentration providing the critical osmotic pressure leading to the following expression for the permeate flux:

$$J = \frac{\Delta P - \Pi_{crit}}{\mu(R_m + R_c)} \tag{2}$$

It is important to control the development of these irreversible fouling layers and to know what filtration operating conditions lead to its formation.

2.3. Critical fouling conditions

Critical fouling can be defined as the process operating conditions leading to the formation of irreversible multilayer fouling on the membrane. The physical meaning of the term critical is used here to relate the irreversible phase transition between a dispersed (reversible concentration polarization) and a condensed phase (irreversible multilayer deposit).

When running a filtration process, several parameters determine the occurrence of the phase transition at the membrane surface, these critical parameters being different when operating in cross-flow or in dead-end mode.

2.3.1. Cross-flow

In cross-flow filtration, a steady state critical flux can be found below which no irreversible fouling occurs [2,3]. However, this critical flux is dependent on another operating condition: the cross-flow velocity. Critical conditions can then be defined with the pair of the following operating parameters: permeate flux and cross-flow velocity. For a given cross-flow velocity, a critical permeate flux can be defined [17,18] or, for a given permeate flux a critical cross-flow velocity exists [17]. So, a critical ratio of permeate flux over the wall shear stress [18] or a critical Peclet number [16] has been theoretically and experimentally introduced to account for this double effect. The critical pair of operating conditions can then be defined as the product of the permeate flux, J, and the mass boundary layer thickness, δ (function of the cross-flow velocity): $(J\delta)_{crit}$.

2.3.2. Dead-end

Since dead-end filtration implies a continual transient state, a steady critical flux concept as deduced from cross-flow filtration cannot be directly applied. Furthermore, it is commonly accepted that for particles, a deposit forms as soon as filtration begin (cake filtration approach), but, Petsev et al. [12] have theoretically shown that when filtering charged colloidal particles in the dead-end mode at a given moment (called the critical time) the coagulation of particles at the membrane surface occurs: the hydrodynamic force acting on the first layer of particles at the membrane overcome the repulsive interaction between particles caused by their charges. A model developed to evaluate reversibility in dead-end operations [8] shows that the formation of a compact irreversible layer occurs for a critical value of the pair "permeate flux and accumulated mass" (accumulated mass being proportional to the filtered volume or to a critical time [12], for constant flux operation). For a given filtered volume, a critical permeate flux can be defined or for a given permeate flux there exists a critical filtered volume. The product of the deposited mass, m, and the permeate flux was found to be critical: $(Jm)_{crit}$. These results led to the optimisation of cleaning procedures (backwashes or flushes) improving the efficiency of filtration operations.

The following paper proposes a procedure allowing the determination of critical fouling conditions for deposit formation in dead-end processes through the measurement of a critical filtered volume for a given permeate flux. The experiments are carried out on suspensions of latex and of clays. The analyse through fouling resistance leads to the definition of an associated parameter for the description of the transition by way of the critical osmotic pressure which links the degree of fouling reversibility to process operating conditions.

3. Materials and methods

3.1. Feed suspensions

Two types of feed suspensions were used: a suspension with well known particle properties (latex suspension), as a basis for a better understanding of the phenomena occurring during dead-end filtration, and a clay suspension to come closer to actual water treatment worries.

3.1.1. Latex

A latex suspension made with monodisperse spherical PVC particles was used and diluted with 10^{-3} M KCl in distilled water to reach 0.02 wt.% (corresponding to 0.0144 vol.%). In these conditions the particles are dispersed: the critical coagulation concentration was found in a previous study [17] to be larger than 0.1 M of KCl. This concentration corresponded to a turbidity of 160 NTU. Particle size distribution was measured with a laser granulometer Zêtasizer 4 (Malvern, Worcestershire, UK). The average latex diameter was 120 nm for the ionic strength used. The pH of the solution was between 6 and 7 corresponding to a zeta potential of -71 mV with an associated error of 2 mV (after correction with the relationship of O'Brien et al. 1978) [11].

3.1.2. Clay

The clay suspension was made of platelet-shaped bentonite particles (the larger dimension is about a hundred times greater than the thickness). The primary clay solution was obtained by dispersing 30 g l^{-1} of osmosis-purified water (Millipore) followed by four repeated sedimentations (each lasting 4 h) to produce stable suspensions. The resulting concentration was about 17 g l^{-1} containing micron sized colloidal particles with a mean hydrodynamic diameter centred on 700 nm [19]. This suspension was then diluted with 10^{-3} M KCl in distilled water (well below the critical coagulation concentration found at 10^{-2} M in KCl [19]) to obtain a 0.02 g l^{-1} concentration, corresponding to 6.5 NTU. This suspension without any buffering then typically displayed a pH between 6 and 7 corresponding to a corrected zeta potential of around -41 mV [20].

3.2. Filtration rig

The experiments were carried out with a bench-scale unit (Fig. 1) using inside-out hollow fibre made of cellulose acetate (Aquasource, Toulouse, France) having a low molecular weight cut-off implying no internal fouling or pore blocking with previously presented feed suspensions.

To avoid contamination of the clean water (used to measure initial permeability), the ultrafiltration module was fed separately with osmosis-purified water (clean water tank) or with the suspension studied (suspension tank).

A volumetric pump ensures a constant flux during the dead-end filtration experiment. Pressure transducers (0–5 bar, Keller) were used to monitor the inlet and outlet pressure, as
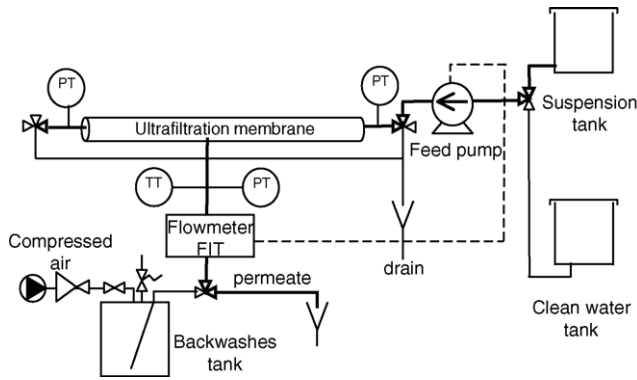
Fig. 1. Schematic of the filtration bench scale unit.

well as the permeate pressure. The permeate flow was measured using an electromagnetic flowmeter (COPA XE Bailey Fischer & Porter). A temperature transducer was situated on the permeate pipe. All parameters were recorded every 30 s via a computer. Operating conditions and membrane characteristics are summarized in Table 1.

3.3. Processing

Formation of an irreversible layer was identified using a succession of filtration periods and discontinuous rinses. The aim of the rinsing step was to remove the reversible accumulated layer. The residual resistance remaining after the rinse was then assumed to be the resistance of the deposit formed during the previous filtration period.

3.3.1. Filtration

Filtrations were carried out with a constant given flux. Firstly, the flux was adjusted using RO-purified water (clean water tank): the initial permeability of the clean module (Lp_0) at the reference temperature of $20\,^\circ C$ can then be checked:

$$Lp_0(20\,^\circ C) = \frac{J}{\Delta P_0} \frac{\mu(T)}{\mu(20\,^\circ C)} \qquad (3)$$

where μ is the viscosity at the experimental temperature (T) or at the reference temperature ($20\,^\circ C$) and the transmembrane pressure (ΔP_0) is taken as the average of the inlet and outlet pressures minus the permeate pressure. Then, the feed was switched to the suspension tank indicating the beginning of the filtration test. After filtration for a given time (corresponding to a filtered volume V_f) a rinse was performed.

Table 1
Hollow fibre properties and operating conditions

Membrane working length (m)	1.12
Fibre internal diameter (mm)	0.94
Number of fibres	21
Total membrane area (m^2)	0.07
Molecular cut-off (kDa)	80
Initial permeability at $20\,^\circ C$ ($l\,h^{-1}\,m^{-2}\,bar^{-1}$)	250
Permeate flux ($l\,h^{-1}\,m^{-2}$)	From 50 to 140

Table 2
Rinse characteristics

Feed flow ($l\,h^{-1}$)	5.6
Internal passage area (m^2)	1.46×10^{-5}
Internal volume (m^3)	1.63×10^{-5}
Velocity (m s^{-1})	0.105
Shear rate (Pa)	0.9
Reynolds	98
Volume of the rinse	$10 \times$ internal volume

3.3.2. Rinsing step

Rinses were run by opening the valve at the outlet of the module, with a chosen frequency defined by the specific volume in $l\,m^{-2}$ filtered between each rinsing step (V_f). As critical fouling conditions are defined as the first deposition of colloids on the membrane [21], rinses have to be run in well-defined conditions (Table 2). In order to avoid erosion of the deposit by shearing, rinses were run at very low flow and a large volume was circulated in the module, with a single passage, to ensure the removal of dispersed particles in a polarization concentration.

The whole experiment corresponded to a total volume produced of $250\,l\,m^{-2}$ leading, in the worst case, to losses in raw water through rinsing steps smaller than 7%. By performing rinses after filtering progressively increasing volumes the idea is to detect the first irreversible gel or deposit layer at the membrane (Section 4.3).

4. Experimental results

Reversibility of fouling was measured by a set of experiments where rinses were processed after the filtration of different volumes of suspension as described in the previous section. Filtration/rinse cycles are first presented in terms of variation of relative permeability along the cycle (Section 4.1) used to deduce a residual resistance after the rinsing steps (Section 4.2). The evolution of this residual resistance with the filtered volume shows the presence of a critical filtered volume (Section 4.3).

4.1. Evolution of permeability along filtration/rinse cycles

In order to show the appearance of a possible drift in permeability, the evolution of relative permeabilities, defined as the ratio between instantaneous (Lp) and initial permeability (Lp_0), was plotted versus filtered volume all along the filtration/rinse experiments.

4.1.1. Latex

Experiments of latex filtration were performed for two different fluxes: 80 and $110\,l\,h^{-1}\,m^{-2}$ and for each flux with at least three different filtered volumes per cycle. Fig. 2 presents the influence of the filtered volume between rinsing steps on the evolution of the relative permeability for
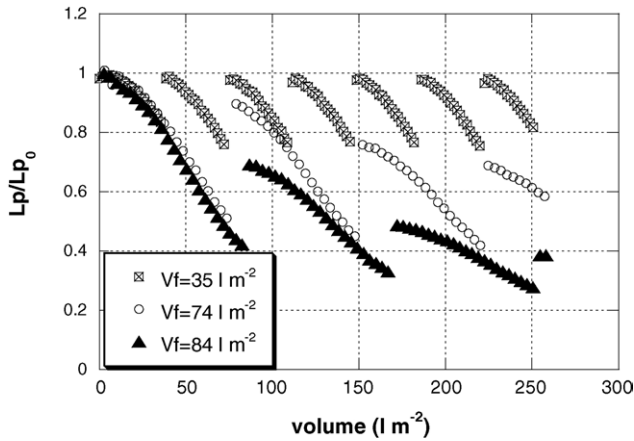
Fig. 2. Evolution of relative permeability Lp/Lp_0 during filtration/rinse cycles for different filtered volumes during the filtration step V_f, latex suspension $0.2\,\mathrm{g\,l^{-1}}$, $J = 110\,\mathrm{l\,h^{-1}\,m^{-2}}$, $Lp_0 = 255\,\mathrm{l\,h^{-1}\,m^{-2}\,bar^{-1}}$ at $20\,^\circ$C.

three volumes between 35 and $84\,\mathrm{l\,m^{-2}}$ for the largest flux.

When the filtered volume per cycle V_f was only $35\,\mathrm{l\,m^{-2}}$, the relative permeability was recovered after each rinsing step, indicating that no irreversible fouling had occurred during the filtration period. When the filtered volume was increased up to 74 and $84\,\mathrm{l\,m^{-2}}$, a drift in the specific permeability was observed leading to a loss of about 10% and 20%, respectively, after each rinse. This is indicative that irreversible fouling (possibly due to particle deposition) was able to occur within the filtration period.

4.1.2. Clay suspension

The same protocol was used to study reversibility on the clay suspension, using imposed fluxes of 50 and $80\,\mathrm{l\,h^{-1}\,m^{-2}}$. Fig. 3 shows the result when the flux was $80\,\mathrm{l\,h^{-1}\,m^{-2}}$ and the filtered volume between rinses increased from 35 up to $91\,\mathrm{l\,m^{-2}}$.

The same general observations as for latex can be made for the clay suspension results: a drift in permeability rapidly
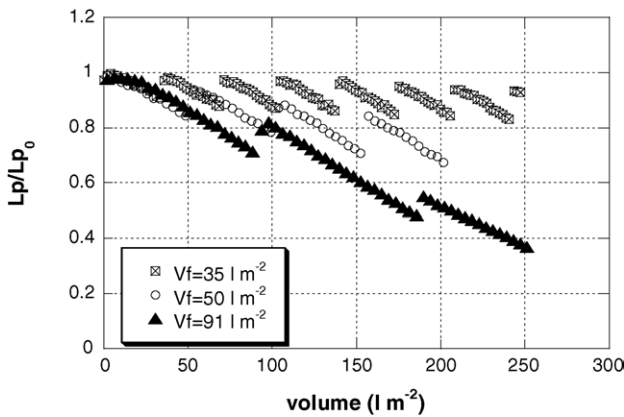

Fig. 3. Evolution of relative permeability Lp/Lp_0 during filtration/rinse cycles for different filtered volumes during the filtration step V_f, clay suspension $0.02\,\mathrm{g\,l^{-1}}$, $J = 80\,\mathrm{l\,h^{-1}\,m^{-2}}$, $Lp_0 = 255\,\mathrm{l\,h^{-1}\,m^{-2}\,bar^{-1}}$ at $20\,^\circ$C.
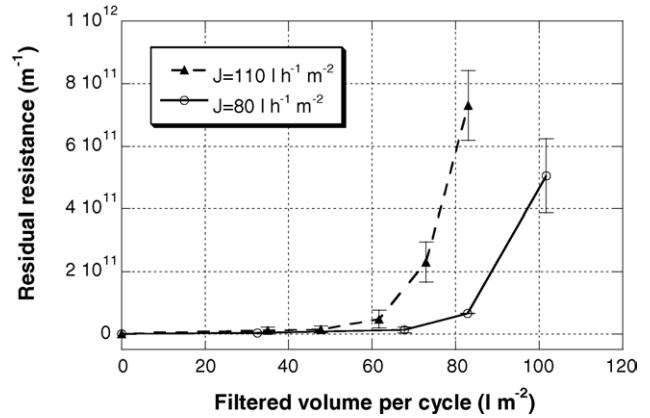

Fig. 4. Variation of the residual resistance with the filtered volume at each latex filtration cycle for two different permeate fluxes. Error bars correspond to the variations observed for the different cycles in the same test.

occurred when increasing the volume filtered between rinsing steps going from 2% to 21% lost per cycle for filtered volume V_f of 35 and $91\,\mathrm{l\,m^{-2}}$, respectively.

4.2. Residual resistance versus filtered volume

In order to analyse these results, a residual resistance, R_{res}, is defined as the difference between the resistance remaining at the beginning of a new cycle $(R_{ci})_n$ and the resistance at the beginning of the previous cycle $(R_{ci})_{n-1}$. For a series of filtration/rinse cycles, the residual resistance is taken as the averaged value of that calculated over the two first cycles, the residual resistance being almost constant along cycles. This residual resistance is plotted in Figs. 4 and 5 for latex and bentonite, respectively, versus the filtered volume between each rinsing step and for the different permeate fluxes. The standard deviation of the residual resistance around the averaged value for the two first cycles is plotted in this graph as error bars.

In Fig. 4, the curves present a similar trend for the different fluxes studied and two periods can be easily identified:
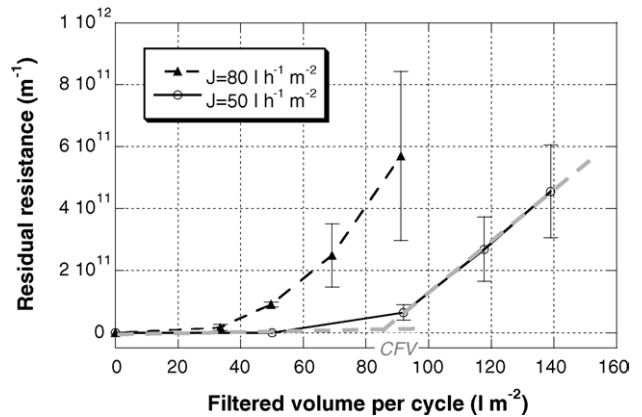

Fig. 5. Variation of the residual resistance with the filtered volume at each clays filtration cycle for two different permeate fluxes. Error bars correspond to the variations observed for the different cycles in the same test.
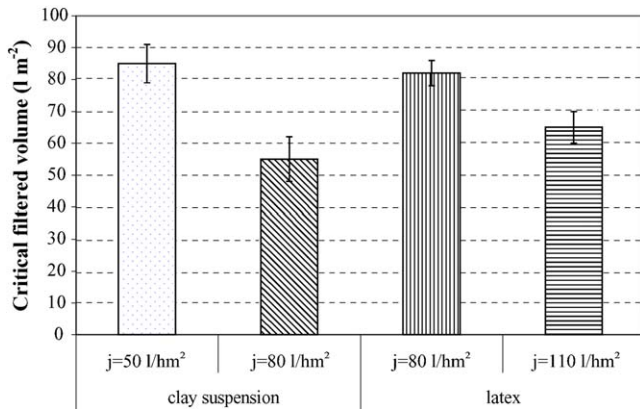
Fig. 6. Critical filtered volume vs. operating flux and suspension.

- the first part, up to 60 and $85 \, l \, m^{-2}$ for 110 and $80 \, l \, h^{-1} \, m^{-2}$, respectively, during which the residual resistance is still negligible;
- the second part, where a dramatic increase in the residual resistance occurs.

The results obtained during filtration of the bentonite suspension (Fig. 5) present the same trends, however the discontinuity is less abrupt and the limit between fouling and non-fouling conditions is fuzzier. Actually, the increase observed in the residual resistance with the filtered volume is about 50% slower than the increase rate observed for the latex suspension.

4.3. Critical filtered volume (CFV)

The critical filtered volume (CFV) is determined by taking the intersection of the tangents of the two parts of the curve as shown in Fig. 5 which represents the variation of the residual resistance (remaining after a rinse) as a function of the volume filtered in the previous filtration cycle. The CFV then corresponds to the limit between fouling and non-fouling conditions. Fig. 6 and Table 3 summarize the critical filtered volumes obtained with the experiments presented previously. In this way, it can be shown (Fig. 6) that the critical accumulated volume is dependent both on the flux and on the kind of suspension studied. Thus, previous research on critical deposition of colloid suspensions showed that critical conditions (such as critical flux in cross-flow) are fully

linked to the suspension stability: critical flux is lower for an increase in ionic strength (and thus reduced repulsive interactions between particles) in the same suspension [8]. It seems clear here that deposits occur for a smaller filtered volume (for a given flux) for bentonite suspensions: at $80 \, l \, h^{-1} \, m^{-2}$ the critical filtered volume is around $55 \, l \, m^{-2}$ for clays and $82 \, l \, m^{-2}$ for latex. Furthermore, the clay is ten times more dilute than the latex suspension (see Section 3.1); the normalization using the mass bulk concentration (C_b), as shown in Table 3, leads to a more discriminating parameter: the critical accumulated mass (CFV $\times C_b$).

The experimental results obtained confirmed the existence of a suitable parameter highlighted by Harmant and Aimar [8] to describe critical fouling conditions in dead-end operations: $(J \times CFV)_{crit}$ or $(J \times CFV \times C_b)_{crit}$ when using the critical accumulated mass (second and last column in Table 3, respectively). Indeed this parameter seems to be suitable to characterise the membrane/suspension combination as it was found to be roughly constant for a given suspension and equal to $4325 \pm 1.2\%$ for the clay and $6850 \pm 4.4\%$ for the latex (Table 3). This parameter can be considered as a criterion for the stability of the suspension: the higher its value the more stable the dispersion (see later on Section 6.2).

The criticality between non-fouling and fouling is pronounced when filtering latex dispersions but less marked for clays. This behaviour could be explained by the idea of a distribution in critical fouling conditions for large colloids, induced by the difference of shape and the wide size distribution of the bentonite particles. The concept can then slip from critical fouling conditions with the existence of no fouling conditions towards sustainable fouling conditions where fouling can occur but is minimised to reduce its impact on the operation.

5. Interpretation of critical filtration conditions in terms of critical osmotic pressure

The experimental results presented in the previous section are now analysed in terms of osmotic pressure and hydraulic deposit resistance, phenomena which are respectively related to concentration polarisation and deposition mechanisms (for background see Sections 2.1 and 2.2). In order to shed light on the transition between concentration polarization and cake

Table 3
Critical conditions in terms of filtered volume and accumulated mass for the two suspensions studied

	Accumulated filtered volume		Accumulated mass	
	CFV ($l \, m^{-2}$)	$J \times$ CFV ($l^2 \, h^{-1} \, m^{-4}$)	CFV $\times C_b$ ($g \, m^{-2}$)	$J \times$ CFV $\times C_b$ ($l \, g \, h^{-1} \, m^{-4}$)
Clay				
$J = 50$	85	4250	1.8	90
$J = 80$	55	4400	1.1	88
Latex				
$J = 80$	82	6560	16.4	1312
$J = 110$	65	7150	13.0	1430

formation, the first part of the filtration results (where the cake does not form) is explained in terms of osmotic pressure (Section 5.1). A critical osmotic pressure is then determined from filtration/rinse experiments (Section 5.2) and later used to characterise the transition between polarisation and deposition during filtration (Section 5.3).

5.1. Method for interpretation of experimental results

Filtration experiments are interpreted by considering consecutive fouling steps:

- *Step* A. In the first part of a filtration run, before any possible cake formation, transfer resistance is due to concentration polarization; the flux is limited by the osmotic pressure at the membrane Π_m, corresponding to Eq. (1) for a fully retentive membrane.
- *Step* B. When concentration at the membrane increases sufficiently to provoke the destabilization of particles, i.e. when osmotic pressure at the membrane, Π_m, reaches a critical value, Π_{crit}, a deposit forms on the membrane providing an additional irreversible resistance (R_c). If a deposit is currently forming, the concentration of polarised particles then remains constant and is associated with a critical osmotic pressure (Π_{crit}): the maximum osmotic pressure reachable in the polarisation concentration. The flux is then given by Eq. (2).
- *Step* C. Just after a rinse, assuming that the rinse volume is sufficient to entirely remove the polarised particles, the osmotic pressure is reduced to the osmotic pressure of the bulk (here ignored). However, a residual resistance, R_{res} can remain.

Even if, from a physical point of view, the flux is described by different equations (Eqs. (1) and (2)), from a mathematical point of view it is possible to consider the same filtration law accounting for an "osmotic pressure like" term [22]:

$$J = \frac{\Delta P - \Pi_m}{\mu R_m} \tag{4}$$

which has a different meaning according to the filtration step:

- *step* A: Π_m is the osmotic pressure
- *step* B: Π_m is the combination of the critical osmotic pressure and a cake resistance:

$$\Pi_m = \Pi_{crit} + J\mu R_c \tag{5}$$

- *step* C: Π_m is relative to the residual resistance persisting after the rinsing step:

$$\Pi_m = J\mu R_{res} \tag{6}$$

In Eq. (4), it should be noted that Π_m represents an osmotic pressure (thermodynamically reversible) when Π_m is lower than Π_{crit} (step A) whereas when Π_m is above Π_{crit} (step B) it is relative to a compressive pressure in a solid phase: the "over-osmotic pressure", $\Pi_m - \Pi_{crit}$ represents the pressure
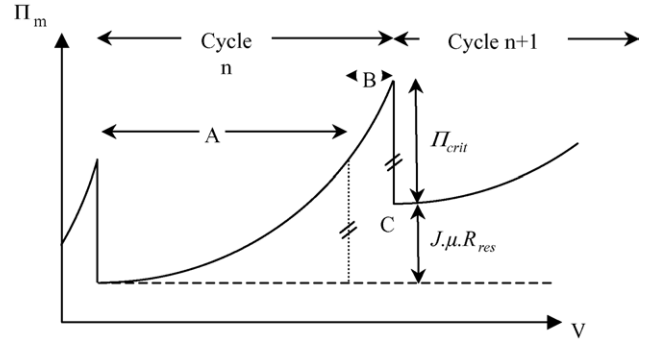

Fig. 7. Variation of Π_m (where $\Pi_m = \Delta P - \Delta P_0$ based on Eq. (4)) vs. the volume V for constant flux operation. Interpretation with a critical osmotic pressure Π_{crit} and a residual resistance R_{res}.

drop in the cake layer. In order to reflect these different characters, Π_m can generally be considered as the solid pressure [23] at the membrane.

If plotting the solid pressure, Π_m defined as the difference between the instantaneous transmembrane pressure (ΔP) and the initial transmembrane pressure (ΔP_0) relative to the clean membrane and the operating flux, as a function of filtered volume along filtration steps A, B and C (Fig. 7), the residual hydraulic resistance of cycle $n+1$ ($R_{res})_{n+1}$, appears to be linked to the residual solid pressure (Eq. (6)) which can then be written as a difference of transmembrane pressures:

$$(R_{res})_{n+1} = \frac{(\Delta P_i)_{n+1} - (\Delta P_i)_n}{\mu J} \tag{7}$$

where $(\Delta P_i)_n$ and $(\Delta P_i)_{n+1}$ represent the initial transmembrane pressure of cycle n and $n+1$, respectively.

The critical osmotic pressure can be easily deduced from Fig. 7 as being the solid pressure removed during the rinsing step. It is then possible to determine the value of Π_{crit} for the cycle n as the difference of transmembrane pressure just before and after the rinsing step:

$$(\Pi_{crit})_n = (\Delta P_f)_n - (\Delta P_i)_{n+1} \tag{8}$$

where $(\Delta P_f)_n$ refers to the final transmembrane pressure of cycle n, or more strictly

$$(\Pi_{crit})_n = \left[\frac{(\Delta P_f)_n}{(\mu J_f)_n} - \frac{(\Delta P_i)_n}{(\mu J_i)_{n+1}} \right] (\mu J_f)_n \tag{9}$$

when taking into account the slight variation in temperature and flux during the experiment.

5.2. Determination of critical osmotic pressure

One can now easily determine the value of Π_{crit} corresponding to each cycle from the initial and final transmembrane pressure of a filtration cycle. The values found for each cycle (Table 4) are almost constant and make it possible to determine, by numerical optimisation on all cycles, a single value of Π_{crit} describing the whole filtration/rinse cycles experiment.

Table 4

Determination of critical osmotic pressure, Π_{crit} and its associated residual resistance, R_{res}, from an experiment: latex, $J = 110\,l\,h^{-1}\,m^{-2}$, $V_f = 84\,l\,m^{-2}$ between rinses (Fig. 2)

	Cycle no.							
	0		1		2		3	
	i	f	i	f	i	f	i	f
ΔP (kPa)	45.2	97.9	61.6	122.8	84.5	143.2	102.2	–
$(\Pi_{crit})_n$ (kPa)		39.8		40.1		38.2		
R_{res} (m^{-1})		6.2×10^{11}		8.4×10^{11}		7.4×10^{11}		

The averaged Π_{crit} values determined for the different volumes and fluxes are reported in Tables 5 and 6 for latex and clay filtrations, respectively.

For a given suspension, values of critical osmotic pressure determined for different operating conditions (filtered volume and applied permeate flux) appear to be almost the same except when the filtered volume is close to the critical filtered volume resulting in low residual resistance (footnote b in Tables 5 and 6). If we do not take into consideration the values corresponding to low residual resistances (lower than 5% of the clean membrane resistance), several observations can be made on the critical osmotic pressure results: whereas the critical filtered volume was found dependent on the permeate flux, the critical osmotic pressure is here independent of operating conditions. Then, the value of critical osmotic pressure Π_{crit} found for the clay suspension is lower than that experimentally determined for latex suspensions highlighting that this parameter is only relative to the suspension/membrane set (discussed in Section 6.2).

5.3. Filtration interpretation with critical osmotic pressure

Furthermore, such an approach allows dissociation of these different fouling mechanisms during the filtration step. When assuming that residual resistance after rinsing corresponds to the deposit formed during the previous filtration period (absence of erosion during the rinsing step), it is possible to depict the different contributions of fouling in terms of cake resistance and osmotic pressure. Table 7 presents equations used for the first cycle and then generalized to a filtration cycle n: these contributions are described below (concentration polarization at the membrane surface) and above (growth of the deposit) Π_{crit} using the light and dark parts, respectively. The same colour code will be used in Fig. 8 to describe the increase in concentration of the dispersed phase and the growth of the deposit.

It should be noted that the value of the critical osmotic pressure then allows the variation of the pressure to be described along the filtration/rinse cycle. Indeed, the equations presented in Table 7 make it possible to split the global resistance into (reversible) osmotic pressure and (irreversible) cake formation contributions, plotted versus filtered volume in Fig. 8: during the first part of the filtration the particles reaching the membrane are accumulated in a dispersed phase (A); they cause an additional resistance to transfer through their osmotic pressure (Π_m) increasing with the concentration, i.e. with the filtered volume. When the volume fraction of the dispersed phase reaches its maximum value, a deposit starts forming (B) whereas the osmotic contribution remains constant at its maximum reachable value (Π_{crit}). Then, rinsing allows depolarization of the accumulation (C). When fil-

Table 5

Critical osmotic pressure, Π_{crit}, deduced from filtration/rinse cycles experiments for the latex suspension

	Latex								
	$J = 80\,l\,h^{-1}\,m^{-2}$				$J = 110\,l\,h^{-1}\,m^{-2}$				
Filtered volume (l m^{-2})	34	70	85	103	35	49	62	75	84
Π_{crit} (kPa)	–[a]	–[a]	27[b]	40	–[a]	–[a]	34[b]	40.3	40

[a] No irreversibility observed.

[b] Weak irreversibility observed.

Table 6

Critical osmotic pressure, Π_{crit}, deduced from filtration/rinse cycles experiments for the clay suspension

	Bentonite							
	$J = 50\,l\,h^{-1}\,m^{-2}$				$J = 80\,l\,h^{-1}\,m^{-2}$			
Filtered volume (l m^{-2})	50	91	120	140	34	50	70	91
Π_{crit} (kPa)	–[a]	5.9	5.9	6.0	3.5[b]	4.5[b]	5.6	6.0

[a] No irreversibility observed.

[b] Weak irreversibility observed.

Table 7
Calculation of the contribution of osmotic pressure and cake in the global resistance

		Initial	General	Final	
		$\Pi_m < \Pi_{crit}$		$\Pi_m > \Pi_{crit}$	
Cycle 0	Cake resistance	$(R_{ci})_0 = 0$	$(R_c)_0 = 0$	$(R_c)_0 = \frac{\Delta P - \Pi_{crit}}{\mu J} - R_m$	$(R_{cf})_0 = \frac{(\Delta P_f)_0 - \Pi_{crit}}{\mu J} - R_m$
	Osmotic pressure	$(\Pi_i)_0 = 0$	$(\Pi)_0 = \Delta P - \mu J R_m$	$(\Pi)_0 = \Pi_{crit}$	$(\Pi_f)_0 = \Pi_{crit}$
Cycle n	Cake resistance	$(R_{ci})_n = \frac{(\Delta P_i)_n}{\mu J} - R_m$	$(R_c)_n = \frac{(\Delta P_i)_n}{\mu J} - R_m$	$(R_c)_n = \frac{\Delta P - \Pi_{crit}}{\mu J} - R_m$	$(R_{cf})_n = \frac{(\Delta P_f)_n - \Pi_{crit}}{\mu J} - R_m$
	Osmotic pressure	$(\Pi_i)_n = 0$	$(\Pi)_n = \Delta P - \mu J(R_m + (R_{ci})_n)$	$(\Pi)_n = \Pi_{crit}$	$(\Pi_f)_n = \Pi_{crit}$

tration carries on as before, the increase in concentration of the dispersed phase appears at the deposit/suspension interface (step A′).

6. Discussion

Here, we discuss the consequences of the critical filtered volume and its associated critical osmotic pressure on how to interpret filtration data (Section 6.1), to characterise the stability of a suspension in regard to its filtration (Section 6.2), and to operate dead-end filtration (Section 6.3).

6.1. Critical osmotic pressure and fouling lag

The determination of Π_{crit} can be considered as a new way of characterising fouling, being complementary to the classical fouling index. The fouling index or fouling potential are relative to the hydraulic resistance of a deposit during the cake filtration phase (the intensity of the fouling) whereas the critical filtered volume and its associated critical osmotic pressure are relative to a fouling lag during which fouling is reversible then being indicative of the poten-

tial of the membrane/suspension system to resist the formation of irreversible fouling (a kind of no-fouling potential). These characterisations of fouling are then complementary as schematically presented in Fig. 9 by plotting the residual resistance versus filtered volume. The slope of the residual resistance over filtered volume after the critical value can then be considered as relative to irreversible fouling and is directly linked to the specific resistance of the irreversible deposit (α) whereas the intercept point is linked to the fouling lag.

The determination of the fouling lag and its associated critical osmotic pressure can then give information on the ability of the membrane/suspension system to stand up to the formation of irreversible fouling (cake or gel) which will be seen in the next section as linked to the stability properties of the suspension. It should be noted that this fouling lag could be the cause for the existence of a critical filtration time which has been experimentally determined during sludge filtration in submerged membrane bioreactors [24,25]. When working below the critical flux in such processes, the concentration at the membrane surface can continue to grow, leading after a critical filtered volume (or a critical time), to the formation of a cake resistance and then to a sudden permeability loss.
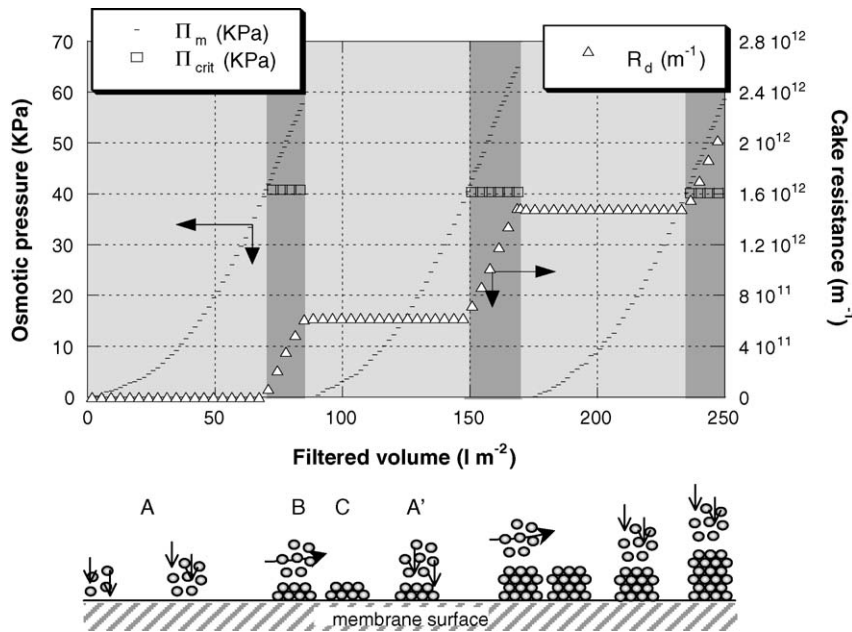

Fig. 8. Schematic of experimental filtration/rinse cycle (latex, $J = 110 \, \mathrm{l \, h^{-1} \, m^{-2}}$, $V_f = 84 \, \mathrm{l \, m^{-2}}$) by dissociating the contribution of osmotic pressure and cake resistance.
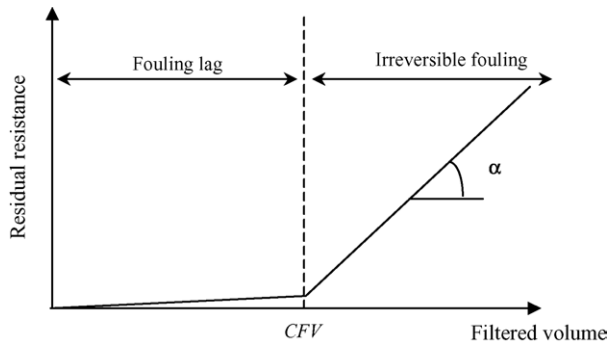
Fig. 9. Residual resistance vs. filtered volume. Fouling lag (and its associated CFV and Π_{crit}) appears to be a means to characterise fouling, being complementary to the classic determination of cake specific resistance, α.

6.2. Critical osmotic pressure and suspension stability characterisation

It has been clearly shown in Section 4 that when different suspensions (latex and clay particles) are filtered with a given permeate flux, the experimentally determined critical filtered volumes are different. The critical osmotic pressure, Π_{crit}, used to interpret these experiments (Section 5) is then different: around 6 kPa for the clay suspension and 40 kPa for the latex suspension.

Such results are in good agreement with theories accounting for surface interactions in transport phenomena [13] since the clay suspension is less stable than the latex suspension: this is confirmed by measurements of zeta potential presented in the Materials section which is lower for clays (−41 mV) than for latex suspension (−71 mV). These high charges on latex particles lead to large repulsive interaction that can explain the high value of the critical osmotic pressure: the pressure needed to irreversibly aggregate the latex dispersion is high.

Critical osmotic pressure is then found to be relative to the suspension stability with regard to filtration. The determination of Π_{crit} could be an interesting tool to classify the fouling characteristics of the suspension in relation to the membrane used.

6.3. Consequences on operating dead-end filtration processes

The determination of critical conditions by filtration/rinse experiments leads to essential keys to run optimized dead-end filtrations: it is observed that, for a defined suspension/membrane set, a working zone can be defined where it is possible to avoid – or at least to greatly limit – irreversible fouling. This working zone can be defined by the operating conditions: the permeate flux, J, and the filtered volume per filtration cycle, CFV (Fig. 10). Below the dashed curves in this figure (corresponding to a critical value of the product $J \times$ CFV) fouling is totally reversible and it can be possible to work with cycles of filtration and rinses. Above this
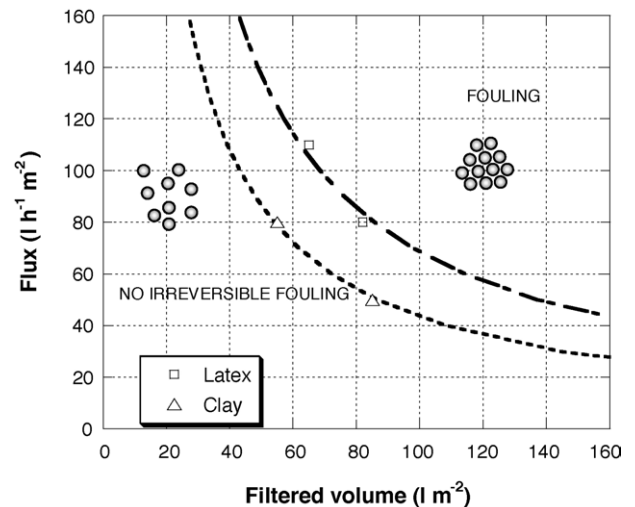

Fig. 10. Chart for determining the optimized working zone: squares represent the latex suspension, triangles represent the clay suspension—dashed curves represent the extrapolation when considering $J \times$ CFV constant.

dashed line, irreversible fouling appears which then requires back flushing to recover permeability. It is important to note that the critical filtered volume decreases when increasing the permeate flux: increasing the permeate flux reduces the possibility to work without irreversible fouling.

For a given working flux, it is possible to reduce the global production cost: indeed the right choice of a "cleaning" frequency corresponding to a filtered volume slightly below the critical value allows the removal of additional resistance by actions requiring low energy (rinsing phases). Such a way to run the process can be seen as sustainable since fouling is reduced to its minimum (above these conditions, an irreversible deposit forms on the membrane surface implying the need for expensive mechanical or even chemical actions).

It is clear that the border between no fouling and fouling conditions becomes less sharp as suspensions become increasingly disperse (in composition and size) as already discussed in Section 4.2. However, a similar trend with the appearance of significant fouling above a critical filtered volume has also been observed during dead-end filtration of natural organic matter using constant pressure operation [26]. Below this critical filtered volume, the reduction of flux due to mass accumulation is instantaneously reversible showing the possibility of the application of this concept to the "real world" of membrane processes. Actually, even when considering a complex fluid, such as natural surface water, likely to add more fouling phenomena (compared to model suspensions) such as adsorption or pore blocking, one can expect critical conditions to exist.

7. Conclusion

The work presented in this paper contributes to the development of sustainable dead-end filtration operations: indeed,

it has been clearly shown experimentally that periodic rinses can be sufficient to avoid a drift in permeability when they are carried out before the formation of the irreversible layer (Fig. 10). This is an important point to investigate for the development of dead-end units as it leads to savings of energy compared with the use of regular backwashes.

The precise determination of the limits between the different fouling mechanisms is then essential to run filtration operations as it can provide indications about the operating parameters suitable to work in the reversible fouling zone. Such a limit is defined by a critical osmotic pressure (which is indicative of a liquid/solid transition at the membrane surface); its experimental determination could be a useful tool for process optimisation. This parameter was found to be almost independent of operating conditions and so suitable for the description of the suspension: the critical osmotic pressure is determined at 40 and 6 kPa, respectively, for latex and clay particles. The associated critical filtered volume is shown to be closely related to the permeate flux: for example for latex particles, permeate fluxes of 80 and $110 \, \mathrm{l \, h^{-1} \, m^{-2}}$ result in CFVs of 82 and $65 \, \mathrm{l \, m^{-2}}$, respectively. An interesting perspective is to use this tool on a real suspension, such as natural surface water where the mechanisms of fouling are more complex on account of the diversity of compounds in terms of shape, size and charge.

Acknowledgments

References

[1] K. Parameshwaran, A.G. Fane, B.D. Cho, K.J. Kim, Analysis of microfiltration performance with constant flux processing of secondary effluent, Water Res. 35 (2001) 4349–4358.

[2] R.W. Field, D. Wu, J.A. Howell, B.B. Gupta, Critical flux concept for microfiltration fouling, J. Membr. Sci. 100 (1995) 259–272.

[3] P. Bacchin, P. Aimar, V. Sanchez, Model for colloidal fouling of membranes, AIChE J. 41 (1995) 368–376.

[4] D.Y. Kwon, S. Vigneswaran, Influence of particle size and surface charge on critical flux of crossflow microfiltration, Water Sci. Technol. 38 (1998) 481–488.

[5] I.H. Huisman, E. Vellenga, G. Trägårdh, C. Trägårdh, The influence of the membrane zeta potential on the critical flux for cross-flow microfiltration of particle suspensions, J. Membr. Sci. 156 (1999) 153–158.

[6] S.S. Madaeni, The effect of operating conditions on critical flux in membrane filtration of latexes, Process. Saf. Environ. Protect. 75 (B4) (1997) 266–269.

[7] G. Belfort, R.H. Davis, A.L. Zydney, The behaviour of suspensions and macromolecular solutions in cross flow microfiltration, J. Membr. Sci. 96 (1994) 1–58.

[8] P. Harmant, P. Aimar, Coagulation of colloids retained by porous wall, AIChE J. 42 (1996) 3523–3532.

[9] V. Chen, A.G. Fane, S. Maedeni, I.G. Wenten, Particle deposition during membrane filation of colloids: transition between concentration polarization and cake formation, J. Membr. Sci. 125 (1999) 109–122.

[10] W.R. Bowen, P.M. Williams, Obtaining the osmotic pressure of electrostatically stabilised colloidal dispersions from frontal ultrafiltration experiments, J. Colloid Interface Sci. 233 (2001) 159–163.

[11] B. Espinasse, Approche théorique et expérimentale de la filtration tangentielle de colloïdes: flux critique et colmatage, PhD Thesis, Université Paul Sabatier, Toulouse, 2003.

[12] A.-S. Jönsson, B. Jönsson, Ultrafiltration of colloidal dispersion—a theoretical model for the concentration polarization phenomena, J. Colloid Interface Sci. 180 (1996) 504–518.

[13] A.S. Michaels, New separation technique for the CPI, Chem. Eng. Prog. 64 (1968) 31–43.

[14] S.K. Zaidi, S.K. Karode, D. Kirpalani, A. Kumar, A new method for identifying osmotically limited and gel layer controlled pressure independent flux in ultrafiltration, Can. J. Chem. Eng. 82 (2004) 343–348.

[15] D.N. Petsev, V.M. Starov, I.B. Ivanov, Concentrated dispersions of charged colloidal particles: sedimentation, ultrafiltration and diffusion, Colloids Surf. A 81 (1993) 65–81.

[16] P. Bacchin, D. Si-Hassen, V. Starov, M.J. Clifton, P. Aimar, A unifying model for concentration polarization, gel-layer formation and particle deposition in cross-flow membrane filtration of colloidal suspensions, Chem. Eng. Sci. 57 (2002) 77–91.

[17] B. Espinasse, P. Bacchin, P. Aimar, On an experimental method to measure critical flux in ultrafiltration, Desalination 146 (2002) 91–96.

[18] G. Gesan-Guiziou, E. Boyaval, G. Daufin, Critical stability conditions in cross flow microfiltration of skimmed milk: transition to irreversible deposition, J. Membr. Sci. 158 (1999) 211–222.

[19] P. Bacchin, P. Aimar, V. Sanchez, Influence of surface interaction on transfer during colloid ultrafiltration, J. Membr. Sci. 115 (1996) 49–63.

[20] C. Causserand, K. Joven, P. Aimar, M. Meireles, Modification of clay cake permeability by adsorption of protein, J. Membr. Sci. 137 (1997) 31–44.

[21] J.A. Howell, Sub-critical flux operation of microfiltration, J. Membr. Sci. 107 (1995) 165–171.

[22] M. Elimelech, S. Bhattacharjee, A novel approach for modelling concentration polarization in crossflow membrane filtration based on the equivalence of osmotic pressure model and filtration theory, J. Membr. Sci. 145 (1998) 223–241.

[23] P. Bacchin, M. Meireles, P. Aimar, Modelling of filtration: from the polarized layer to deposit formation and compaction, Desalination 145 (2002) 139–146.

[24] B.D. Cho, A.G. Fane, Fouling transients in nominally sub-critical flux operation of a membrane bioreactor, J. Membr. Sci. 209 (2002) 391–403.

[25] S. Ognier, C. Wisniewski, A. Grasmick, Membrane bioreactor fouling in sub-critical filtration conditions: a local critical flux concept, J. Membr. Sci. 229 (2004) 171–177.

[26] Y. Bessiere, P. Bacchin, B. Jefferson, Dead-end filtration of natural organic matter: experimental evidence of critical conditions, Desalination, FCF'04, in press.